AIP | Applied Physics Letters

Gapless band structure of PbPdO2: A combined first principles calculation and experimental study

S. W. Chen, S. C. Huang, G. Y. Guo, J. M. Lee, S. Chiang, W. C. Chen, Y. C. Liang, K. T. Lu, and J. M. Chen

Citation: Applied Physics Letters **99**, 012103 (2011); doi: 10.1063/1.3607293
View online: http://dx.doi.org/10.1063/1.3607293
View Table of Contents: http://scitation.aip.org/content/aip/journal/apl/99/1?ver=pdfcov
Published by the AIP Publishing

Gapless band structure of $PbPdO_2$: A combined first principles calculation and experimental study

S. W. Chen,[1] S. C. Huang,[2] G. Y. Guo,[2,3,a)] J. M. Lee,[1] S. Chiang,[4] W. C. Chen,[5] Y. C. Liang,[1] K. T. Lu,[1] and J. M. Chen[1,a)]
[1]*National Synchrotron Radiation Research Center, Hsinchu 30076, Taiwan*
[2]*Department of Physics, National Taiwan University, Taipei 10617, Taiwan*
[3]*Graduate Institute of Applied Physics, National Chengchi University, Taipei 11605, Taiwan*
[4]*Department of Chemical Engineering, Rensselaer Polytechnic Institute, Troy, New York 12180, USA*
[5]*Instrument Technology Research Center, National Applied Research Laboratories, Hsinchu 30076, Taiwan*

(Received 16 May 2011; accepted 13 June 2011; published online 5 July 2011; publisher error corrected 20 July 2011)

We present experimental evidence of the gapless band structure of $PbPdO_2$ by combined x-ray photoemission and x-ray absorption spectra complemented with first principles band structure calculations. The electronic structure near the Fermi level of $PbPdO_2$ is mainly composed of O 2*p* and Pd 4*d* bands, constructing the conduction path along the Pd-O layer in $PbPdO_2$. Pd deficiency in $PbPdO_2$ causes decreased O 2*p*-Pd 4*d* and increased O 2*p*-Pb 6*p* hybridizations, thereby inducing a small band gap and hence reducing conductivity. Hall measurements indicate that $PbPdO_2$ is a p-type gapless semiconductor with intrinsic hole carriers transporting in the Pd-O layers. © *2011 American Institute of Physics*. [doi:10.1063/1.3607293]

Materials can be broadly classified into metals, insulators, semiconductors, and half metals, depending on their electronic band structures. If the conduction and valence band edges meet at the Fermi level, the material belongs to a new class of solids named zero-gap materials or gapless semiconductors. There are only a few known gapless semiconductors which are made of Hg-based II-VI compounds.[1,2] They were well studied in near-infrared absorption/emission[2–4] and also room temperature ferromagnetism used for spintronics.[5,6] However, these materials are toxic and easily oxidized. Recently, Wang[7] theoretically proposed $PbPdO_2$ with a zero-gap band structure to be the first oxide-based gapless semiconductor. With the unique band structure, physical properties of $PbPdO_2$ are very sensitive to external influences, such as pressure or magnetic field, or internal forces, such as chemical inhomogeneity.[7,8] For example, with Co doping, $PbPdO_2$ exhibits a gapless feature between the majority spins in the conduction band and the minority spins in the valence band.[8] By controlling the Fermi level with applied electric field, electrons with 100% spin polarization can be obtained. Co-doped $PbPdO_2$, a so-called spin gapless semiconductor, can be a promising material for spintronics applications. $PbPdO_2$ thus could be a suitable matrix to develop new material systems.

To develop a new material with a desired band structure, based on $PbPdO_2$ matrix, it is essential to understand its electronic structure, particularly near the Fermi level. However, experimental evidence of zero-gap characteristic and detailed electronic stricture of $PbPdO_2$ is scarce. As well established, x-ray absorption spectroscopy (XAS) and photoemission spectroscopy (PES) can probe the unoccupied and occupied density of states above/below the Fermi level of materials, respectively. In this study, we combined XAS and PES spectra[9] complemented with first-principles electronic structure calculations to provide a detailed investigation on the electronic structure of gapless semiconductor $PbPdO_2$ with various stoichiometry. Results provide a fundamental understanding of gapless band structure of $PbPdO_2$ that can be a basis to design new material systems with novel physical properties, by tuning its band structure, in the fields of magnetism,[8,10] optics, electronics,[8] and spintroics.

Bulk $PbPdO_2$ samples were prepared by the solid state method using β-PbO and PdO as starting materials.[11,12] Two pellets, after synthesized, were further annealed at 150 °C for 24 and 36 hours in the atmosphere of $N_2 + 5\%H_2$ to remove oxygen atoms. All $PbPdO_2$ samples were identified as orthorhombic structures by the x-ray diffraction measurement. PES and XAS spectra of $PbPdO_2$ were collected at the high energy spherical grating monochromator (HSGM) beamline in the National Synchrotron Radiation Research Center in Taiwan. All measurements were processed in an ultra high vacuum (UHV) chamber. As collecting O *K*-edge XAS spectra, the spectrum of a CuO single crystal was measured simultaneously in a separate chamber, which enabled us to achieve energy calibration better than 0.02 eV accuracy. The energy resolution of the monochromator was set to about 0.15 eV at the O K-edge. PES signals were collected by the VG Microtech CLAM 4MCD analyzer system excited with a photon energy of 650 eV. The incident photon energy calibration was made by recording the kinetic energy of the Au 4f levels. The Fermi level of the samples was referred to that of a gold foil electrically contacted with the sample. To avoid the surface contamination and probe the electronic structure precisely, a pellet of $PbPdO_2$ was cleaved within the UHV chamber to obtain a clean surface and manifest the bulk electronic structure as measurement.

Theoretical band structure of $PbPdO_2$ is obtained by first principles calculations with projector augmented-wave (PAW) method,[13] as implemented in the Vienna ab initio

a)Authors to whom correspondence should be addressed. Electronic mail: jmchen@nsrrc.org.tw; gyguo@phys.ntu.edu.tw.

simulation package (VASP).[14,15] These calculations are based on density functional theory (DFT)[16] with the generalized gradient approximation (GGA)[17] plus on-site Coulomb interaction U. The effective U (Ref. 18) used for Pd 4d orbitals is 2 eV. The structural optimizations were carried out using the cut-off energy of 500 eV for plane waves and $8 \times 8 \times 12$ Monkhorst-Pack k-point grid in the Brillouin zone. The energy convergence criterion was set to 10^{-6} eV. The equilibrium structures were obtained when the forces acting on all the atoms were less than 0.02 eV/Å. The total and partial densities of states were calculated using a finer $10 \times 20 \times 20$ k-point grid.

Figure 1(a) shows a valence-band photoemission spectrum combined with an O K-edge XAS spectrum of $PbPdO_2$, in which valence-band PES spectrum is related in energy to the Fermi level of the samples, the position of the valence band maximum (VBM) is given by the intercept of the gradient of the highest occupied bands with the energy axis. The XAS spectrum is also aligned with respect to the Fermi level of the PES data, by correlating the O 1s PES binding energy scale relative to the Fermi level to the O 1s XAS photon energy scale, as the same approach adopted in references (Refs. 19–21). The position of the conduction band minimum (CBM) is extracted using the same gradient method, as applied to the VBM determination, which is widely used for extracting band offsets.[22] As shown in Fig. 1(a), VBM and CBM touch at the Fermi level, indicating the gapless characteristic of $PbPdO_2$.

To characterize the corresponding band structure, we present the calculated density of states of $PbPdO_2$ in Figs. 1(b) and 1(c). Fig. 1(b) shows the total density of states of $PbPdO_2$ that satisfactorily reproduces the overall features of the present valence-band PES spectrum and the fine structure of the O K-edge XAS spectrum shown in Fig. 1(a). The conduction band minimum and valence band maximum touch at the Fermi level (E_F) ($E_F = 0$ eV), as supported by XAS and PES spectra in Fig. 1(a), evidencing the gapless band structure of $PbPdO_2$. Fig. 1(c) displays the decomposed density of states of O 2p, Pd 4d, and Pb 6p bands of $PbPdO_2$, respectively. The occupied bands ~1.7 eV below E_F and unoccupied bands ~0.8 eV above E_F are dominated by Pd 4d bands, whereas those ~3 eV above E_F exhibit predominantly Pb 6p characters. This indicates that the electronic structure of $PbPdO_2$ near the Fermi level is mainly composed of Pd 4d and O 2p hybridized bands.

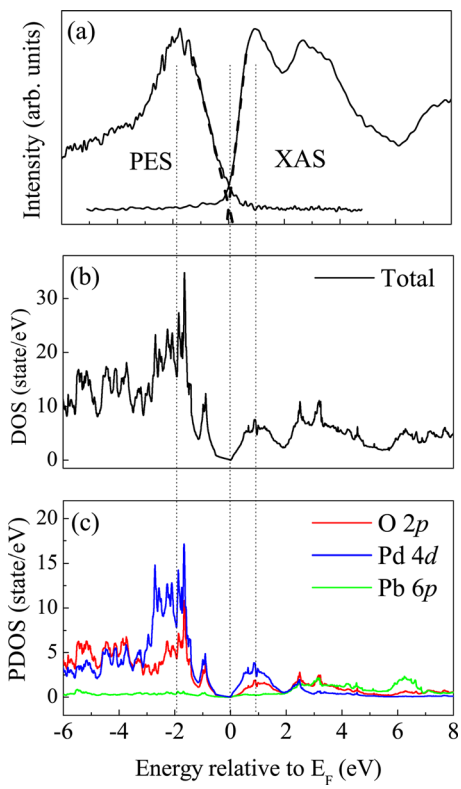

FIG. 1. (Color online) (a) Valence-band photoemission and O K-edge x-ray absorption spectra of $PbPdO_2$. (b) Calculated total density of states (DOS). (c) Decomposed partial density of states (PDOS) of O 2p, Pd 4d, and Pb 6p bands.

Because the electronic structure of $PbPdO_2$ near the Fermi level is predominantly composed of the O 2p-Pd 4d hybridized bands, the band structure of $PbPdO_2$ should be very sensitive to the stoichiometry of Pd and O atoms. We thus probed the O K-edge absorption spectra of the O- and Pd-deficient $PbPdO_2$ samples. In Figure 2, O K-edge x-ray absorption spectra of Pd-deficient $PbPdO_2$ were reproduced. We note that the absorption edge of O K-edge spectra of Pd-deficient $PbPdO_2$ progressively shifts to higher energy with decreasing Pd concentration, implying a small band gap formed, in contrast to the original zero band gap. Meanwhile, the intensity of the main pre-peak decreases and an additional peak sited at the energy ~534.5 eV forms in the O K-edge absorption spectra of the Pd-deficient $PbPdO_2$ samples. According to the band structure calculations as shown in Fig. 1, the pre-peak ~530.2 eV in the O K-edge spectrum represents the hybridization between the O 2p and Pd 4d bands, and the additional peak at ~534.5 eV corresponds to the formation of the hybridization between the O 2p and Pb 6p bands. Therefore, Fig. 2 clearly demonstrates that Pd deficiency in $PbPdO_2$ enhances the hybridization of the O 2p band with the Pb 6p band but notably reduces that between the O 2p and Pd 4d bands.

We also probe the O K-edge x-ray absorption spectra of the O-deficient $PbPdO_2$ samples as shown in Figure 3. No up-shift of the absorption edge in the O K-edge spectra of O-deficient $PbPdO_2$ was observed, indicating $PbPdO_2$ remained

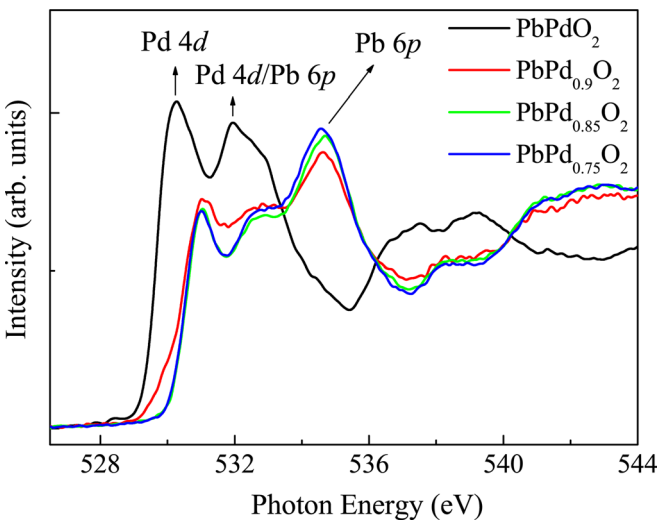

FIG. 2. (Color online) O K-edge x-ray absorption spectra of Pd-deficient $PbPdO_2$.

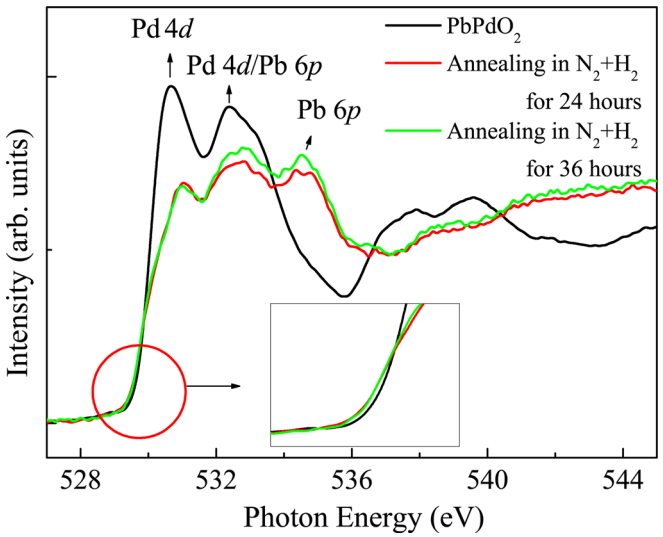

FIG. 3. (Color online) O *K*-edge x-ray absorption spectra of O-deficient $PbPdO_2$. Inset shows pre-edge region of O *K*-edge spectra.

its gapless band structure. As seen from the inset of Fig. 3, the absorption edge of O *K*-edge absorption spectrum of $PbPdO_2$ shifts to lower energy as oxygen atoms were removed. This implies that O-deficient $PbPdO_2$ causes the oxygen defect state formed on the bottom of conduction band, inducing a tailing of the conduction band minimum, as proposed in the oxygen-deficient semiconductor such as TiO_2 (Refs. 23 and 24). In Figure 3, we also observe the decreased intensity of the main pre-peak at ~530.6 eV and an additional peak formed at 534.5 eV, reflecting the weakened hybridization between the O 2*p* and Pd 4*d* bands and the strengthened one between the O 2*p* and Pb 6*p* bands in O-deficient $PbPdO_2$.

Table I shows the transport properties measured by I-V and Hall measurements of the $PbPdO_2$ samples annealed in reduced atmospheres. Clearly, the conductivity of Pd- and O-deficient $PbPdO_2$ decreases as compared with the parent $PbPdO_2$. $PbPdO_2$ with an orthorhombic structure is composed of Pb-O and Pd-O layers stacked as the layer-by-layer structure.[11,12] The O 2*p* and Pd 4*d* hybridized band forms the electronic structure of $PbPdO_2$ near the Fermi level as well as the conduction path along the Pd-O layer. Pd or oxygen deficiency in $PbPdO_2$ samples, leading to the weakened hybridization between O 2*p* and Pd 4*d* bands, will destroy this conduction path. The conductivity of Pd- and O-deficient $PbPdO_2$ thus decreases as evidenced by I-V measurements shown in Table I. Table I only shows the resistivity of O-deficient $PbPdO_2$, because the resistivity of Pd-deficient $PbPdO_2$ is too high to be measured. The drastic decrease in the conductivity of Pd-deficient $PbPdO_2$ is attributed to the formation of a band gap as evidenced in Fig. 2. The Hall measurements indicate the p-type properties of $PbPdO_2$, implying hole carriers transporting along the conductive path.

TABLE I. Measured resistivity (ρ), carrier mobility (μ), and carrier concentration (n) of $PbPdO_2$ annealed in reduced atmospheres.

Sample	$PbPdO_2$	$PbPdO_2$ annealed in $N_2 + H_2$ for 24 h	$PbPdO_2$ annealed in $N_2 + H_2$ for 36 h
ρ (Ω-cm)	0.623	1.407	2.469
μ (cm^2/V-s)	4.597	3.223	1.324
N (10^{18}/cm^{-3})	5.587	3.681	2.022

In conclusion, we present a combined experimental and theoretical study on the electronic structure of gapless semiconductor $PbPdO_2$. The electronic structure of $PbPdO_2$ near the Fermi level is mainly composed of O 2*p* and Pd 4*d* hybridized bands, constructing the conduction path along the Pd-O layer in the orthorhombic structure of $PbPdO_2$. Hall measurements indicate $PbPdO_2$ being a p-type gapless semiconductor with intrinsic hole carriers transporting in the Pd-O layers. Pd deficiency in $PbPdO_2$ enhances the hybridization between the O 2*p* and Pb 6*p* bands but reduces notably that between the O 2*p* and Pd 4*d* bands, causing a small band gap formed. O/Pd deficiency, destroying the conduction path, causes the diminished conductivity of $PbPdO_2$. The present study evidences the gapless band structure of $PbPdO_2$ and elucidates its detailed electronic structure and intrinsically conductive properties. The results could help to design new material systems, based on the $PbPdO_2$ matrix, with unique band structure and novel physical properties.

We thank the NSRRC staff for their technical support and the National Science Council of Republic of China for the financial supports.

[1]E. M. Sheregii, J. Cebulski, A. Marcelli, and M. Piccinini, Phys. Rev. Lett. **102**, 045504 (2009).
[2]A. M. Witowski and J. K. Furdyna, Phys. Rev. B **48**, 10855 (1993).
[3]W. D. Hu, X. S. Chen, F. Yin, Z. J. Quan, Z. H. Ye, X. N. Hu, Z. F. Li, and W. Lu, J. Appl. Phys. **105**, 104502 (2009).
[4]A. Witowski, K. Pastor, and J. K. Furdyna, Phys. Rev. B **26**, 931 (1982).
[5]H. Krenn, W. Zawadzki, and G. Bauer, Phys. Rev. Lett. **55**, 1510 (1985).
[6]A. Twardowski, H. J. M. Swagten, and W. J. M. de Jonge, Phys. Rev. B **42**, 2455 (1990).
[7]X. L. Wang, Phys. Rev. Lett. **100**, 156404 (2008).
[8]X. Wang, G. Peleckis, C. Zhang, H. Kimura, and S. Dou, Adv. Mater. **21**, 2196 (2009).
[9]K. Horiba, A. Chikamatsu, H. Kumigashira, M. Oshima, N. Nakagawa, M. Lippmaa, K. Ono, M. Kawasaki, and H. Koinuma, Phys. Rev. B **71**, 155420 (2005).
[10]K. J. Lee, S. M. Choo, J. B. Yoon, K. M. Song, Y. Saiga, C.-Y. You, N. Hur, S. I. Lee, T. Takabatake, and M. H. Jung, J. Appl. Phys. **107**, 09C306 (2010).
[11]T. C. Ozawaa, T. Taniguchia, Y. Nagataa, Y. Norob, T. Nakac, and A. Matsushita, J. Alloys Compd. **395**, 32 (2005).
[12]T. C. Ozawa, T. Taniguchi, Y. Nagata, Y. Noro, T. Naka, and A. Matsushita, J. Alloys Compd. **388**, 1 (2005).
[13]P. E. Blöchl, Phys. Rev. B **50**, 17953 (1994).
[14]G. Kresse and J. Hafner, Phys. Rev. B **48**, 13115 (1993).
[15]G. Kresse and J. Furthmüller, Comput. Mater. Sci. **6**, 15 (1996).
[16]P. Hohenberg and W. Kohn, Phys. Rev. **136**, B864 (1964).
[17]J. P. Perdew, K. Burke, and M. Ernzerhof, Phys. Rev. Lett. **77**, 3865 (1996).
[18]S. L. Dudarev, G. A. Botton, S. Y. Savrasov, C. J. Humphreys, and A. P. Sutton, Phys. Rev. B **57**, 1505 (1998).
[19]O. Seifarth, J. Dabrowski, P. Zaumseil, S. Müller, D. Schmeißer, H.-J. Müssig, and T. Schroeder, J. Vac. Sci. Technol. B **27**, 271 (2009).
[20]A. Sandell, P. G. Karlsson, J. H. Richter, J. Blomquist, P. Uvdal, and T. M. Grehk, Appl. Phys. Lett. **88**, 132905 (2006).
[21]P. G. Karlsson, L. I. Johansson, J. H. Richter, C. Virojanadara, J. Blomquist, P. Uvdal, and A. Sandell, Surf. Sci. **601**, 2390 (2007).
[22]F. Capasso and G. Margaritondo, *Heterojunction Band Discontinuities: Physics and Device Applications* (North-Holland, Amsterdam, 1989).
[23]W. Yan, Z. Sun, Z. Pan, Q. Liu, T. Yao, and Z. Wu, Appl. Phys. Lett. **94**, 042508 (2009).
[24]S. W. Chen, J. M. Lee, K. T. Lu, C. W. Pao, J. F. Lee, T. S. Chan, and J. M. Chen, Appl. Phys. Lett. **97**, 012104 (2010).